

PACS numbers: 42.55.Lt; 42.60.Lh; 41.85.Lc
DOI: 10.1070/QE2007v037n02ABEH003416

Electron-beam pumping of excimer media in a multipole magnetic field. 1. Numerical simulation of the energy input

S.V. Arlantsev, K.S. Gochelashvili, O.N. Evdokimova, M.E. Zemskov, G.P. Mkheidze

Abstract. **A scheme of the system for pumping active gas media by electron beams injected into a gas volume located in a multipole magnetic field is proposed and engineering solutions are presented, which were used in the development and making of this system. The possibility of changing a resistance to a plasma current initiated by a relativistic electron beam is promising for the additional control of the kinetics of processes in the active gas medium with the aim of increasing the energy input efficiency. The scheme proposed in the paper allows the combination of the pumping of the gas medium by an electron beam with pumping by a controllable discharge initiated by this beam in electric fields of the beam. The energy input of electron beams to the gas medium located in a quadrupole magnetic field is analysed by the Monte-Carlo method. The calculations demonstrate a high efficiency (90 %) of the beam energy transfer to the gas and the possibility to control the energy-input profile.**

Keywords: *excimer gas lasers, electron-beam pumping, multipole magnetic field.*

1. Introduction

The development of high-power short-wavelength visible and UV coherent radiation sources is of great interest both for fundamental studies in the field of laser fusion and high-density energy physics and many applications [1 – 3]. The main efforts of researchers are concentrated on the creation of electron-beam pumped wide-aperture excimer lasers [4 – 9]. However, the difficulties encountered in the generation of short radiation pulses in active excimer media are well known. In this connection the projects devoted to the development of extremely bright hybrid laser systems with a femtosecond $Ti:Al_2O_3$ master oscillator and a final amplification stage based on an optically pumped excimer medium (a Xe – F amplifier on the blue – green transition pumped by the luminescence of Xe_2 excited by electron beams) were recently extensively discussed [10]. Note that due to the scalability of a gas excimer amplifier, it is possible to achieve the exawatt power level without using a complex and expensive system of chirped pulses, which is employed in solid-state amplifying stages.

The systems for electron-beam pumping of active excimer media available at present do not satisfy, in our opinion, a number of requirements imposed on the optimal system. Among them is first of all the necessity to increase the conversion efficiency of the electron-beam energy to laser radiation energy and the possibility of a controllable combination of the advantages of electron-beam pumping and electric-discharge excitation of the active medium. The pumping system should also provide the possibility of controlling the transverse structure of the laser beam. Therefore, the development of new pumping systems for active gas media, which would satisfy the above-mentioned requirements, remains of current interest.

The scheme for injecting n electron beams into a gas chamber with a multipole (n-fold) magnetic field was considered earlier in [11]. It was shown that, by varying the gas pressure, magnetic field strength, and electron-beam energy (depending on the chamber dimensions), the regime can be selected at which the maximum of the beam energy is utilised in the gas volume.

The studies of the transport of electron beams in gases [12 – 14] have shown that it is possible to control the plasma current induced by a relativistic electron beam in a beam plasma and that the energy input of the plasma current to the gas is large (up to 50 %). This opens up the possibility to combine the advantages of the beam pumping and electric-discharge excitation of the active medium by initiating a homogeneous volume discharge in intrinsic electric fields of the beam.

In this paper, we report the study performed by using a new scheme for pumping active excimer media by injecting counterpropagating electron beams in a quadrupole magnetic field and presents the results of Monte-Carlo simulations of the energy input of electron beams to the gas volume.

The system considered below is intended for increasing the excitation efficiency of the active medium by the two methods: either by increasing the efficiency of energy transfer from electron beams to the working mixture by using a multipole magnetic field or by increasing the efficiency of production of active excimer molecules upon pumping the gas medium simultaneously by the electron beam and a discharge excited by this beam. In this case, the electron-beam-pumped laser operates as a laser on a non-self-sustained discharge maintained by the electron beam.

S.V. Arlantsev State Unitary Enterprise 'V.K. Orlov Granat Development Bureau', Volokolamskoe sh. 95, 123424 Moscow, Russia;
K.S. Gochelashvili, O.N. Evdokimova, M.E. Zemskov, G.P. Mkheidze A.M. Prokhorov General Physics Institute, Russian Academy of Sciences, ul. Vavilova 38, 119991 Moscow, Russia;
e-mail: knst@kapella.gpi.ru

Received 14 January 2005; revision received 24 April 2006
Kvantovaya Elektronika **37** (2) 124 – 129 (2007)
Translated by M.N. Sapozhnikov

2. Experimental setup

The basic components of the laser system, shown schematically in Fig. 1, are fabricated at present. Double forming lines (DFLs) made of standard high-voltage cables are used as pulsed voltage generators [15]. Cable DFLs in the experimental setup provide the required mobility. They are loaded on explosive-emission diodes producing a total current of ~ 150 kA at a voltage of ~ 300 kV. The diodes arranged in five sections (four diodes in each of the sections) provided the control of the beam plasma density. DFLs were charged through inductances L_2 by using a pulsed voltage generator (PVG). A magnetic-field supply battery can produce magnetic fields with the induction $B \sim 0.5$ T in diodes and the laser chamber.

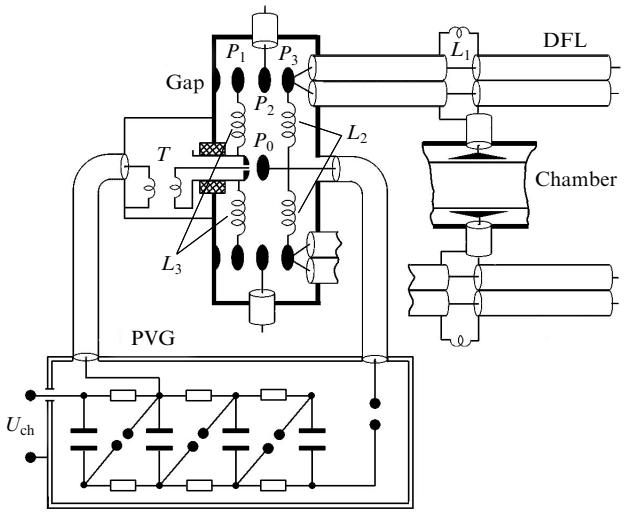

Figure 1. Scheme of the PVG, gap, and DFLs.

When the voltage across a DFL achieves the maximum value, trigatron gap P_0 triggered by a pulse from the PVG comes into action, and as a result a voltage of 300 kV is applied to all the four gaps P_1. The breakdown of these gaps is provided by the decoupling inductances L_3. The operation of gaps P_1 initiates the breakdown of gaps P_2 and P_3 and, hence, the operation of DFLs. Each of the four four-electrode gaps (consisting of P_1, P_2, and P_3) commutes five DFLs. Inductances L_3 prevent the discharge of DFLs through other gaps.

Figure 2a illustrates the principal scheme for DFL charging. The charging of DFLs is described by the expressions (for $C_1 = C_2$)

$$U_{1,2} = B\left[\left(\Omega_2^2 - \delta_{1,2}\right)\cos\Omega_1 t - \left(\Omega_1^2 - \delta_{1,2}\right)\cos\Omega_2 t + \left(\Omega_1^2 - \Omega_2^2\right)\right],$$

where

$$B = \left[\left(1 + \frac{2C_1}{C_0}\right)\left(\Omega_1^2 - \Omega_2^2\right)\right]^{-1};$$

$$\delta_1 = \frac{(C_0 + 2C_1)(C_1 + C_p)}{C_0 C_1 L_0 (C_1 + 2C_p)}; \quad \delta_2 = \frac{C_p(C_0 + 2C_1)}{C_0 C_1 L_0 (C_1 + 2C_p)};$$

$$\Omega_1 = \left[\beta + \left(\beta^2 - \gamma\right)^{1/2}\right]^{1/2}; \quad \Omega_2 = \left[\beta - \left(\beta^2 - \gamma\right)^{1/2}\right]^{1/2};$$

$$\beta = \frac{2C_1C_pL_1 + 2C_0C_1L_0 + C_1^2L_1 + C_0C_pL_1 + C_0C_1L_1}{2C_0C_1L_0L_1(C_1 + 2C_p)};$$

$$\gamma = \frac{C_0 + 2C_1}{C_0C_1L_0L_1(C_1 + 2C_p)}.$$

Because of the presence of the charging inductance L_1, DFLs are charged to different voltages. The relative voltage difference across the lines at a time instant t is

$$\frac{U_1 - U_2}{U_0} = k_0 k(\cos\Omega_1 t - \cos\Omega_2 t),$$

where

$$k_0 = \frac{L_1C_1}{1 + 2C_1/C_0}; \quad k = \frac{\Omega_1^2\Omega_2^2}{\Omega_2^2 - \Omega_1^2}.$$

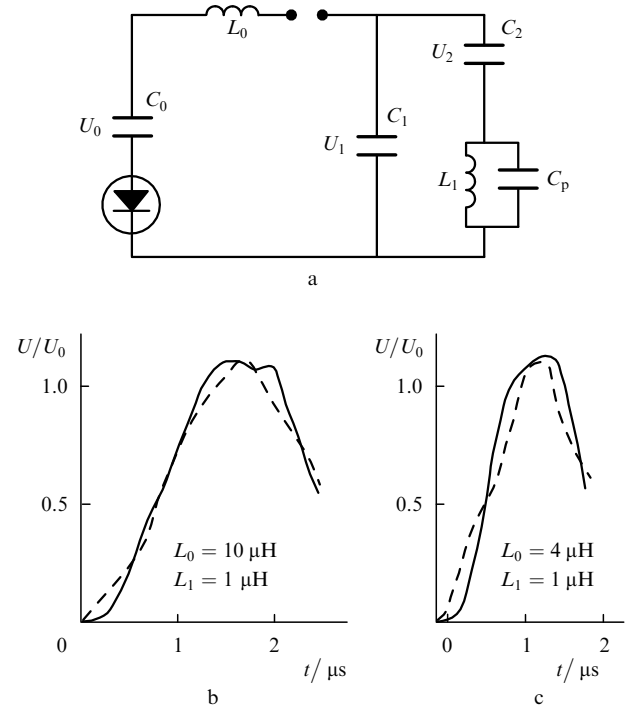

Figure 2. Scheme of DFL charging (a) and time dependences of U/U_0 (b, c): C_0 is the PVG discharge capacity; L_0 is the PVG inductance; C_1 and C_2 are DFL capacities; L_1 is the charging DFL inductance; C_p is the parasitic capacity; U_0 is the PVG voltage.

Figure 2b, c show the time dependences of U/U_0 (U_0 is the voltage across the PVG) for the DFL capacity $C_1 = C_2 = 2.5 \times 10^{-8}$ F (solid curve) and $C_1/C_0 = 0.4$ (dashed curve) for $L_0 = 10$ μH (Fig. 2b) and $L_0 = 4$ μH (Fig. 2c). One can see from these curves that for these values of C and L, DFLs are charged in fact simultaneously.

3. Calculations of fields

Figure 3 presents the sectional views of the diode and chamber. The analytic calculation of a real electric field in the diode is complicated. The field strength on the cathode

was estimated by using the transformation $\omega = \arccosh(r/\varkappa)$. Two equipotentials, which correspond approximately to the contours of the cathode and anode, are shown by the dashed curves in Fig. 3. On the equipotential corresponding to the cathode the values of the relative field strength E/E_0 at several points are given ($E_0 = 79$ kV cm^{-1}). The values of E/E_0 at points a, b, and c are equal to 10, 5.4, and 3.1, respectively. It is obvious that, due to the presence of microscopic apexes on the cathode surface, the effective field exceeds the macroscopic electric field by a factor of κ. As a result, field electron emission from the cathode surface changes to explosive emission already at relatively low electric fields. The current density from the cathode is restricted either by emission (for small E and κ) or the spatial charge.

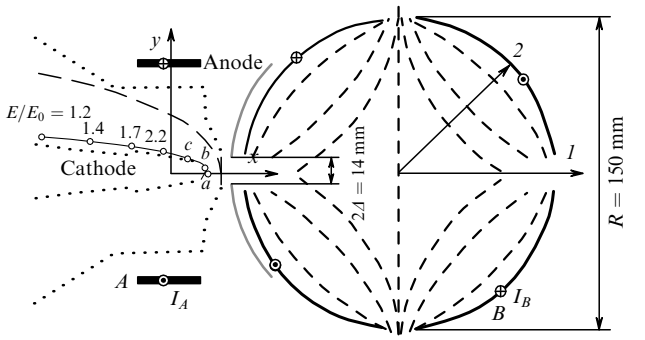

Figure 3. Sectional views of the diode and chamber.

The density of the field-emission current from the cathode at points b and c with respect to the current density at point a is described by the Fowler–Nordheim formula

$$\frac{j}{j_a} = \left(\frac{\varepsilon}{\varepsilon_a}\right)^2 \exp \frac{6.9 \times 10^7 \Phi^{3/2}}{E_0} \frac{\varepsilon - \varepsilon_a}{k\varepsilon\varepsilon_a},$$

where $\varepsilon = E/E_0$ and Φ is the work function of a metal in electronvolts.

A magnetic field required to restrict the electron current from points b and c (located at a distance y from the x axis) by the aperture of the anode foil ($2\Delta = 14$ mm) is

$$B = \left(\frac{mc^2}{e} \frac{\gamma E_\perp}{\rho}\right)^{1/2}.$$

The estimates of fields and currents in the diode are presented in Table 1.

A magnetic field is produced in the system by conductors A and B, whose shape is shown in Fig. 3. By varying current in the conductors, we can change the magnetic field configuration. The magnetic field with the quadrupole configuration increases from its centre to periphery in the interval of radii from 0 to 70 mm. As r further increases, the magnetic field either gradually decreases in direction *1* or drastically increases in direction *2* (to the conductor).

Table 1. Calculation of fields and currents in a diode.

Point	$\varepsilon = E/E_0$	$E_\perp/$ kV cm^{-1}	$\rho = 0.5(\Delta - y)/$mm	B_0/T	j/j_a ($\kappa \approx 300$)
a	10	0	3.5	0	1
b	5.4	300	2.25	0.36	$(2.8 - 29) \times 10^{-2}$
c	3.1	230	0.5	0.64	$(1.2 - 950) \times 10^{-4}$

4. Simulation of the beam energy input to the laser chamber

The optimal parameters of the beam, magnetic field, and gas mixture were determined by Monte-Carlo simulations of the beam energy input to the laser chamber filled with argon at pressures 1–3 atm in the presence of an external quadrupole magnetic field. For simplicity, the calculation was performed for a chamber with a quadratic section.

The geometry of simulations is shown in Fig. 4. The electron beams are injected to the chamber from four sides. In the chamber corners the conductors are located, which produce a multipole (in our case, quadrupole, $n = 4$) magnetic field. The values of the magnetic field presented in Table 2 correspond to the beam injection site. The energy-input profiles for one fourth of the chamber section ($x - y$) are shown in Figs 5–9.

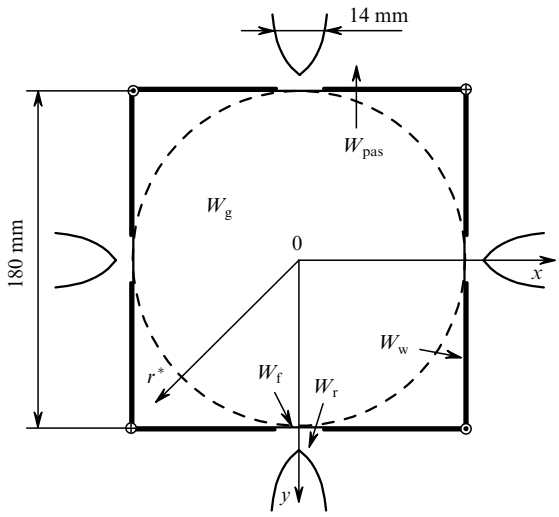

Figure 4. Simulation geometry.

The calculated parameters are presented in Table 2. The energy of 'stopped' electrons (with energies lower than 5 keV) imparted to the gas is not indicated.

Figure 5 presents the distribution of the specific energy input to argon calculated at a pressure of 1.5 atm in the magnetic field $B_0 = 0.05$ T ($E_0 = 300$ keV). The general increase in the beam-energy input to argon in the magnetic field $B_0 = 0.1$ T is approximately 42 % compared to the case when the field is absent. As the magnetic field is increased, the energy input to the gas increases, losses on the walls decrease, and the energy of electrons absorbed in the foil and reflected from it back to the diode weakly changes.

Figure 6 shows the distribution of the specific energy input to gas over the x and r^* axes (see Fig. 4) for $P_0 = 1.5$ atm and $E_0 = 300$ keV. It is obvious that the inhomogeneity of the energy input in the direction r^* should be maximal. One can see from Fig. 6 that for the argon pressure of 1.5 atm and magnetic field of ~ 0.05 T, the

Table 2. Results of numerical calculations.

Gas	P_0/ atm	B_0/T	E_0/ keV	W_0	W_g	W_w	W_f	W_r	W_{pas}
Ar	1.5	0	300	3000	1101	747	364	250	181
	1.5	0.05	300	3000	1296	680	376	246	147
	1.5	0.1	300	3000	1561	440	333	276	132
	2.1	0.05	300	3000	1684	368	376	245	43
	3	0.05	300	3000	1990	78	398	198	0
	3	0.1	300	3000	2080	42	361	245	0
	1	0.1	150	1500	346	0	784	260	0
	1	0.1	300	3000	640	1196	344	192	308
	1	0.3	250	2500	1156	360	428	260	88
	1	0.3	400	4000	1176	1652	296	116	476

Note: W_0 is the energy of an electron beam injected into the chamber (total energy of injected electrons); W_g is the energy imparted to gas in the entire chamber volume (ionisation losses); W_w is the energy of a beam incident on the chamber walls; W_f is the beam energy absorbed in foils of all the four output windows (the titanium foil thickness is 50 μm); W_r is the energy of electrons reflected from the foil back to the diode; W_{pas} is the energy of a beam propagated to the opposite wall of the chamber; energies W are presented in relative units.

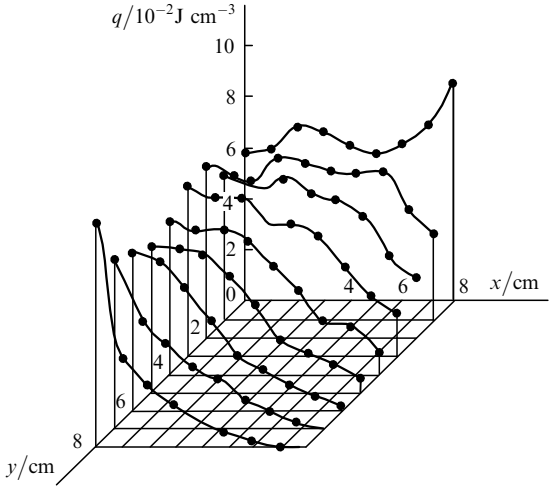

Figure 5. Distribution of the specific energy input for $E_0 = 300$ keV, $P_0 = 1.5$ atm, and $B_0 = 0.05$ T.

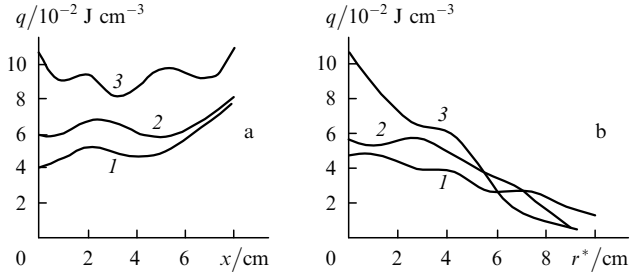

Figure 6. Distribution of the specific energy input to gas over the x (a) and r^* (b) axes for $B_0 = 0$ (*1*), 0.05 (*2*), and 0.1 T (*3*); $E_0 = 300$ keV, $P_0 = 1.5$ atm.

diameter of the region of the relatively homogeneous energy input is ~ 80 mm, i.e. 60 % of the laser aperture.*

*It should be taken into account that in the case of a relatively small amount of probe particles, considerable fluctuations in the calculated values are possible. In the real case, the distributions of the specific energy input will be smoother.

Figure 7 shows the distribution of the energy input for $P_0 = 3$ atm and a magnetic field of 0.05 T ($E_0 = 300$ keV). For these values of pressure and magnetic field, the efficiency of energy transfer from the electron beam to gas achieves ~ 70 %, which provides the specific energy input (within the aperture of diameter ~ 60 mm) approximately equal to 0.08 – 0.1 J cm^{-3}.

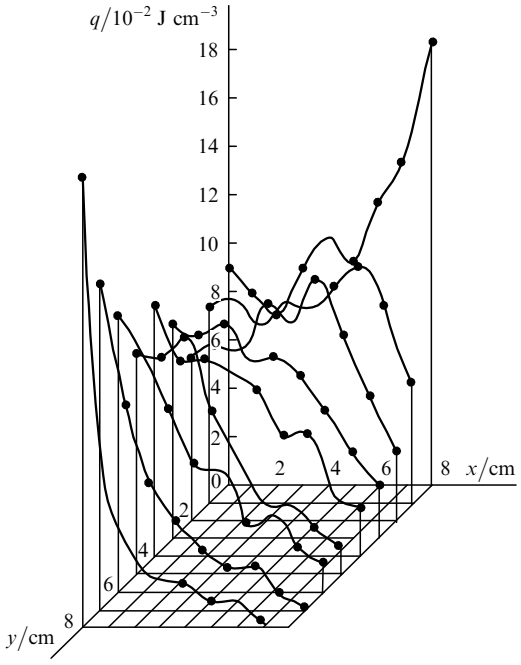

Figure 7. Distribution of the specific energy input for $E_0 = 300$ keV, $P_0 = 3$ atm, and $B_0 = 0.05$ T.

Figure 8 presents the distributions of the energy input over the x and r^* axes in the magnetic field $B_0 = 0.05$ T at pressures $P_0 = 2.1$ and 3 atm. The inhomogeneity of the energy input over the chamber section does not exceed 20 % within the aperture of diameter ~ 60 mm.

Figure 9 shows the radial distributions of the specific energy input for $P_0 = 1$ atm, $B_0 = 0.1$ T, and the electron energy $E_0 = 150$ and 300 keV. In these calculations, the magnetic field was simulated by four segments, each of them consisting of 10 – 30 conductors. Thus, the geometry of

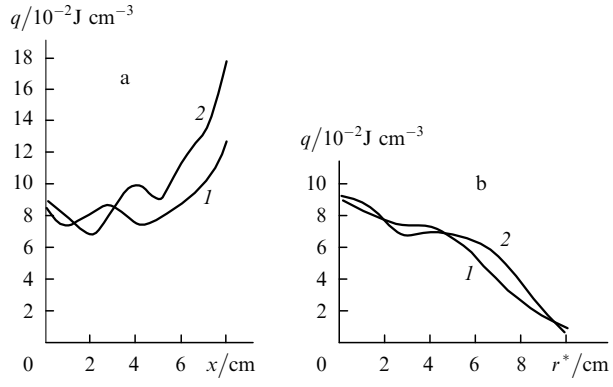

Figure 8. Distribution of the energy input over the x (a) and r^* (b) axes for $P_0 = 2.1$ (*1*) and 3 atm (*2*); $E_0 = 300$ keV, $B_0 = 0.05$ T.

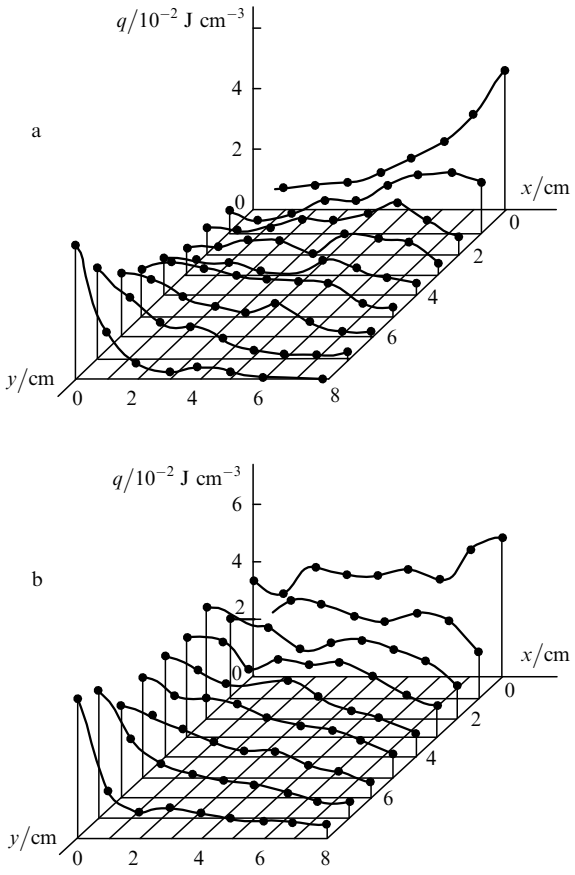

Figure 9. Distribution of the specific energy input for $E_0 = 150$ (a) and 300 keV (b); $P_0 = 1$ atm, $B_0 = 0.1$ T.

simulations corresponded to that of the chamber (see Fig. 3).

The results of simulations show that the beam energy is quite efficiently transferred to the gas in the system under study* and the gas mixture volume and the laser resonator aperture are used completely enough. By varying the mixture pressure, external magnetic field, and electron energy for the specified number of conductors, we can control the distribution of the energy input in the chamber.

5. Plasma currents

The injection region of an electron beam is a one-dimensional (linear) magnetic mirror, and the quadrupole magnetic field represents a magnetic trap. This region is shown schematically in Fig. 10. We will assume that the transverse velocities of electrons emitted from the cathode are negligibly small compared to their longitudinal velocities. The electrons in the beam propagated through a foil acquire transverse velocities $v_\perp$. The electrons for which the ratio of the longitudinal and transverse velocities is

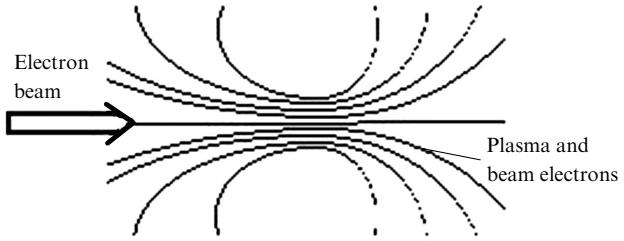

Figure 10. Magnetic mirror in the beam-injection region.

$$\frac{v_\parallel}{v_\perp} \leqslant \left(\frac{B_{\max} - B_{\min}}{B_{\min}}\right)^{1/2}$$

are reflected from the magnetic mirror. It is obvious that for the specified magnetic field it is always possible to find the position of the cathode and foil at which all the electrons emitted from the cathode will enter the laser chamber.

The energy of the beam electrons injected into the chamber with a multipole magnetic field is mainly spent to ionise the gas mixture.

The field induced by the increasing beam current and the field of a spatial charge injected into the chamber generate a plasma current of plasma electrons and beam electrons multiply scattered and reflected from magnetic walls. By manipulating the magnetic field, we can change the relation between the beam injected into the chamber (magnetic trap) and the electron beam escaping from the chamber at the beam current build-up stage, i.e. change the field of a spatial charge in the working chamber. At the stage of the quasi-stationary beam current (on the plateau of the current pulse), the field of the spatial charge in the working chamber can be changed by varying the resistance to the inverse current (by a magnetic field, adding the electronegative gas to the mixture). This allows the control of the relation between the electric field and gas density (E/ρ), i.e. the discharge regime. Therefore, the beam can successfully initiate a homogeneous volume discharge in intrinsic electric fields.*

To obtain lasing, the pump power density should be no less than 10^5 W cm^{-3}. Such a density can be provided both by electron-beam and discharge pumping. It is known that active excimer molecules are produced upon electron-beam and electric-discharge pumping due to various physicochemical reactions. Each of these pumping methods has its own advantages and disadvantages [17]. An attractive idea of combining both these methods in one system in the traditional approach [18] (a system without a magnetic field or with a homogeneous magnetic field) involves a number of difficulties. At the same time, as was shown above, by using a multipole magnetic field, both pumping methods can be simultaneously realised in the system proposed here. In this case, in our opinion, the advantages of both these pumping methods can be combined.

6. Conclusions

We have proposed a new scheme for pumping active excimer media by injecting electron beams into a gas

* Upon injection of electron beams to a chamber with a multipole magnetic field, the efficiency of energy transfer from the beam to the working mixture depends on the degree n of multipolarity of the magnetic field B, the electron energy E_0, the working gas pressure P_0, and the position (diameter) of conductors with current. For the chamber diameter of 150 mm, the optimal efficiency is achieved for $n \approx 12$, $P_0 = 2.5 - 3$ atm, and $E_0 \approx 250$ keV. As B increases, the energy transfer efficiency increases, but for $B > 1$ T, the increase slows down. According to calculations, the maximum efficiency is ~ 0.9.

* The influence of currents induced in a plasma on the emission parameters of an electron-beam-pumped excimer laser was first considered in paper [16].

volume located in a multipole magnetic field and have presented engineering solutions for the development and making of this system.

The efficiency and spatial distribution of the energy input of electron beams injected from four sides to the laser gas medium located in a quadrupole magnetic field have been studied by Monte-Carlo simulations. The results of calculations have demonstrated the possibility of controlling the profile of the energy input to the gas volume in the pumping system proposed and a high efficiency of energy transfer from the electron beam to gas. Experiments performed earlier [12] also demonstrate the important advantage of this system allowing the control of the relation between electron-beam and electric-discharge pumping initiated in the intrinsic fields of plasma currents.

Acknowledgements. This work was partially supported by the Russian Foundation for Basic Research (Grant Nos 05-02-17484a and 05-08-33370a).

References

1. Basov N.G., Krokhin O.N. *Zh. Eksp. Teor. Fiz.*, **46**, 171 (1964).
2. Mesyats G.A. *Impul'snaya energetika i elektronika* (Pulsed Energetics and Electronics) (Moscow: Nauka, 2004); Mesyats G.A., Osipov V.V., Tarasenko V.F. *Pulsed Gas Lasers* (Washington: SPIE Press, 1995).
3. *Zababakhinskie nauchnye chteniya. Trudy VIII konferentsii* (Zababakhin Scientific Readings, Proceedings of VIII Conference) (Chelyabinsk: All-Russian Research Institute of Technical Physics, 2005).
4. Sethian J.D., Pawley C.J., Obenschain S.P., et al. *IEEE Trans. Plasma Sci.*, **25**, 221 (1997).
5. Shaw M.J. *Proc. SPIE Int. Soc. Opt. Eng.*, **3092**, 154 (1997).
6. Owadano Y., Okuda I., Matsumoto Y., et al. *Fusion Engineering and Design*, **44**, 91 (1999).
7. Zvorykin V.D., Arlantsev S.V., Bakaev V.G., et al. *Laser and Particle Beams*, **19**, 609 (2001).
8. Abdullin E.N., Grishin D.M., Gubanov V.P., et al. *Kvantovaya Elektron.*, **34**, 199 (2004) [*Quantum Electron.*, **34**, 199 (2004)].
9. Bugaev S.P., Abdullin E.N., Zorin V.B., et al. *Kvantovaya Elektron.*, **34**, 801 (2004) [*Quantum Electron.*, **34**, 801 (2004)].
10. *Proc. International Conf. Ultrahigh Intensity Lasers* (Cassis, France, 2006).
11. Arlantsev S.V. et al. *Trudy IOFAN*, **45**, 166 (1994).
12. Bondar' Yu.F. et al. Preprint IOFAN, No. 57 (Moscow, 1986); Bondar' Yu.F. et al. *Zh. Tekh. Fiz.*, **58** (5), 884 (1988); Bondar' Yu.F. et al. *Pis'ma Zh. Tekh. Fiz.*, **14** (12), 1116 (1988).
13. Mesyats G.A., Mkheidze G.P., Savin A.A. *Entsiklopedia nizkotemperaturnoi plazmy* (Encyclopaedia of Low-Temperature Plasma). Ed. by V.E. Fortov (Moscow: Nauka, 2000) Vol. 4, pp 108 – 126.
14. Mkheidze G.P. *Entsiklopedia nizkotemperaturnoi plazmy* (Encyclopaedia of Low-temperature Plasma). Ed. by V.E. Fortov (Moscow: Nauka, 2000) Vol. 4, pp 126 – 132.
15. Korop E.D. *Prib. Tekh. Eksp.*, (1), 124 (1981).
16. Mangano J.A., Hsia J., Jacob J.H., Srivastava B.N. *Appl. Phys. Lett.*, **33** (6), 487 (1978).
17. McDaniel I., Nigen W. (Eds) *Gazovye lazery* (Gas Lasers) (Moscow: Mir, 1986).
18. Kushner M.J. *IEEE J. Quantum Electron.*, **26**, 1546 (1990).